Antiferromagnetic Resonance in FeF_2 at Far-Infrared Frequencies*†

R. C. OHLMANN‡ AND M. TINKHAM
Department of Physics, University of California, Berkeley, California
(Received March 13, 1961)

Antiferromagnetic resonance in single crystals of FeF_2 was observed between 1.5° and 66°K ($T_N=78.4$°K) in the far-infrared region. The resonance frequency at $T\approx 0$ was found to be $\nu(0)=52.7\pm 0.2$ cm^{-1}. Using the antiferromagnetic resonance relation derived by Kittel, Nagamiya, Keffer, and others, and using the experimental value for the static susceptibility, the uniaxial anisotropy constant at absolute zero, $K(0)$, was inferred to be 1.1×10^8 ergs/cm^3 (40 cm^{-1}/atom). Measurements of the splitting of the line caused by an external magnetic field gave $g_{\|}=2.25\pm 0.05$. The anisotropy energy in FeF_2, being primarily due to the crystalline field-spin-orbit interaction, may be described by a term $\Sigma_i DS_{zi}^2$ in the Hamiltonian. By including this interaction in the molecular-field treatment, we have determined $D=-9\pm 2$ cm^{-1}, and have calculated the temperature dependences of the sublattice magnetization, the anisotropy constant, the resonance frequency, and the line width. The last two were compared with the experimental results and found to be in reasonable agreement. The linewidths were found to follow a T^4 law above 15°K. The search over a frequency region of 13–70 cm^{-1} for the absorption lines expected in the paramagnetic region was unsuccessful, possibly indicating a relaxation time of less than 10^{-12} sec.

I. INTRODUCTION

ANTIFERROMAGNETIC resonance was predicted by Kittel[1] in 1951, and has been discussed more completely by a number of authors since then.[2–8] It has been shown that the resonance frequency has a direct dependence on both the exchange and anisotropy energies. This fact has made the resonance observations particularly useful, since the magnetic anisotropy of an antiferromagnet is difficult to determine by the usual torque measurements. This difficulty is due to the absence of any externally appearing magnetization, except for the small induced moment, which contains anisotropy effects only in second order.

Various antiferromagnets differ in the magnitude and origin of their anisotropy, as well as in the strength of their exchange interaction, and it is informative to study the resonance absorption in a number of them. The few compounds which have been investigated[9] prior to the present work have been characterized by the fact that their resonance frequencies have been reached using millimeter microwave techniques. However, many antiferromagnets have sufficiently large exchange and anisotropy energies that their resonance frequencies are expected to lie in the submillimeter or far-infrared spectral region. We have observed the antiferromagnetic resonance in FeF_2, which has a very high anisotropy energy, at about 1580 kMc/sec (corresponding to a free-space wavelength of ~ 0.2 mm) at low temperatures. A preliminary account of this work has been previously given.[10]

Ferrous fluoride has a rutile-type structure[11] as shown in Fig. 1. The Fe^{++} ions, which form a body-centered tetragonal structure, are surrounded by a distorted octahedron of six F^- ions. The symmetry axes at a cation site are the [110], [1$\bar{1}$0], and [001] directions. The axes of the body-centered ion are rotated 90° about the c axis to obtain the equivalent axes at a corner ion, thus causing the macroscopic anisotropy to be uniaxial. This anisotropy is relatively strong since it is due to the effect of the symmetry of the crystalline electric field upon the spins through the spin-orbit interaction. Below the Néel temperature of 78.35°K,[12] long-range antiferro-

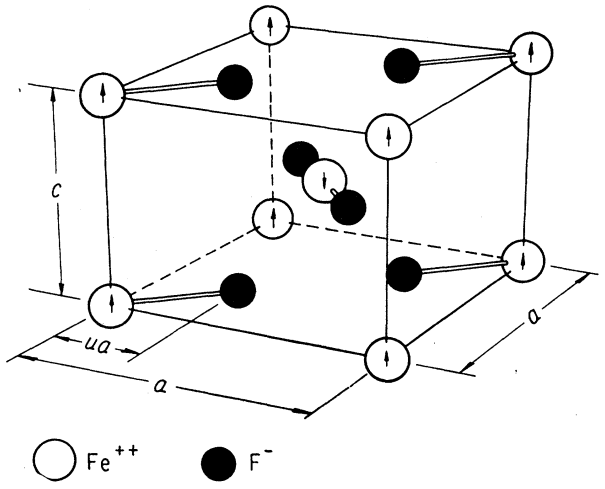

FIG. 1. Crystal structure of FeF_2 showing the magnetic moment arrangement in the antiferromagnetic state. The lattice parameters, from reference 11, are $a=4.6966$ A, $c=3.3091$ A, and $u=0.305$.

* Based on a thesis submitted in partial fulfillment of the requirements for the degree of Doctor of Philosophy by Robert C. Ohlmann, Department of Physics, University of California, Berkeley, California, June, 1960.

† Supported by the National Science Foundation, The Alfred P. Sloan Foundation, and the U. S. Office of Naval Research.

‡ Westinghouse Research Laboratories Fellow, now at Westinghouse Research Laboratories, Pittsburgh 35, Pennsylvania.

[1] C. Kittel, Phys. Rev. **82**, 565 (1951).
[2] T. Nagamiya, Progr. Theoret. Phys. (Kyoto) **6**, 342 (1951).
[3] F. Keffer and C. Kittel, Phys. Rev. **85**, 329 (1952).
[4] K. Yosida, Progr. Theoret. Phys. (Kyoto) **6**, 691 (1952); **7**, 25 (1952); **7**, 425 (1952); **8**, 285 (1952).
[5] C. J. Gorter and J. Haantjes, Physica **18**, 285 (1952).
[6] J. Ubbink, Physica **19**, 9, 919 (1953).
[7] R. K. Wangsness, Phys. Rev. **93**, 68 (1954); **111**, 813 (1958).
[8] E. S. Dayhoff, Phys. Rev. **107**, 84 (1957).
[9] F. M. Johnson and A. H. Nethercot, Phys. Rev. **114**, 705 (1959), and references cited therein.
[10] R. C. Ohlmann and M. Tinkham, Bull. Am. Phys. Soc. **3**, 416 (1958).
[11] J. W. Stout and S. A. Reed, J. Am. Chem. Soc. **76**, 5279 (1954).
[12] J. W. Stout and E. Catalano, J. Chem. Phys. **23**, 1803 (1955).

magnetic order is present and the ions may be grouped into two sublattices according to their average spin directions,[13] as shown in Fig. 1.

II. THEORY

The antiferromagnetic resonance frequency of a two-sublattice antiferromagnet having uniaxial anisotropy, in the absence of an external field, is given by[3]

$$\omega_0=\gamma(2H_EH_A+H_A^2)^{\frac{1}{2}}, \tag{1a}$$

where $\gamma=ge/2mc$, H_E is the exchange field, and H_A is the anisotropy field. This has been derived using a molecular-field approximation in which $H_E=\lambda M$, where λ is the molecular-field constant, and M is the average sublattice magnetization. If the uniaxial anisotropy energy is written in its simplest phenomenological form as

$$E_A=-\tfrac{1}{2}K(\cos^2\theta_1+\cos^2\theta_2),$$

where θ_1 and θ_2 are the angles between the two sublattice magnetizations and the easy (c) axis, then it is also easy to show[14] that $H_A\approx K/M$.

The exchange and anisotropy effects may be separated using the perpendicular susceptibility (in the antiferromagnetic state) and the relation[15] $(\chi_\perp)^{-1}=\lambda+(K/2M^2)$. By substituting into Eq. (1a), the resonance frequency may be written

$$\omega_0=\gamma(2K/\chi_\perp)^{\frac{1}{2}}. \tag{1b}$$

Thus, the anisotropy constant, K, can be calculated from the experimentally measured quantities.

The above theory was derived on the assumption of an isotropic g factor in the gyromagnetic ratio γ. However, the susceptibility measurements on FeF_2 (in the paramagnetic state) show[16,17] that $g_{\parallel}$ is greater than $g_\perp$ by about 10%. The usual isotropic molecular-field approximation is not directly applicable in the case of an anisotropic g value, but the simplicity of the standard approach may be recovered by a transformation to an isotropic form. The manner in which this may be done has been shown by Nagamiya[18] in his treatment of the antiferromagnetic resonance in orthorhombic $CuCl_2\cdot 2H_2O$. Following Nagamiya, we assume an isotropic g value, which we arbitrarily set equal to $g_{\parallel}$. The results of the isotropic theory may then be taken over with the modification that, where the external field $\mathbf{H}$ appears in the equations, its component perpendicular to the c axis is replaced by $(g_\perp/g_{\parallel})H_\perp$, while the perpendicular susceptibility $\chi_\perp$ is replaced by $(g_{\parallel}/g_\perp)^2\chi_\perp$.

The preceding theory is used in Sec. IV to analyze the experimental results. In Sec. V, the theory of the anisotropy energy is discussed on the basis of a spin Hamiltonian-molecular field treatment and its temperature dependence is derived. The linewidth and shape are discussed in Sec. VI, and the paramagnetic region in Sec. VII.

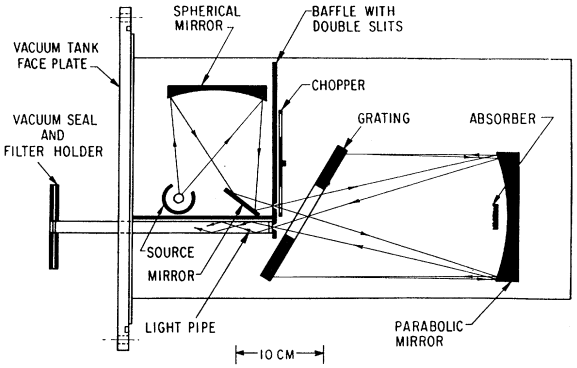

FIG. 2. Schematic diagram of the far-infrared monochromator. The diagonal mirror was usually replaced by a KRS-5 crystal or a zero-order grating.

III. EXPERIMENTAL METHODS

Monochromator

The far-infrared monochromator, schematically shown in Fig. 2, was similar in optical design to the one described by McCubbin and Sinton.[19] The source of radiation was a high-pressure mercury vapor lamp (General Electric type H100-A4). A Littrow system was used, the main diffraction gratings having 2 by 3 in. oval-shaped holes in their centers to allow the use of an on-axis parabolic mirror of $f/1.5$ aperture ratio. The echellete gratings were ruled in the departmental shop either on a $\frac{1}{16}$-in. layer of solder bonded to a brass backing plate, or on solid Dural. They had a 14.5° blaze angle and ruling spacings of 0.26, 0.34, 0.45, and 0.75 mm.

The harmonics of the desired frequency, which were also diffracted and reached the exit slit, were greatly attenuated by a combination of filters. Carbon-black coatings on the mirrors and transmission filters absorbed the near-infrared radiation, while crystal quartz, fused quartz, and rock-salt filters removed most of the longer-wavelength harmonics. In addition, the plane mirror before the entrance slit was replaced either by a crystal of KRS-5, for use from 140 to 280 μ, or by an appropriate zero-order grating, for use at longer wavelengths. The depth of the observed antiferromagnetic resonance absorption showed that a radiation purity of about 90% was obtained at about 190 μ.

An innovation was the use of a metal light pipe[20] to channel the radiation from the exit slit to the liquid-helium Dewar, as shown in Fig. 3. To eliminate the

[13] R. A. Erickson, Phys. Rev. **90**, 779 (1953).
[14] See, for example, T. Nagamiya, K. Yosida, and R. Kubo, *Advances in Physics*, edited by N. F. Mott (Taylor and Francis, Ltd., London, 1955), Vol. 4, p. 1.
[15] J. H. Van Vleck, J. Chem. Phys. **9**, 85 (1941).
[16] J. W. Stout and L. M. Matarrese, Revs. Modern Phys. **25**, 338 (1953).
[17] S. Foner (private communication).
[18] T. Nagamiya, Prog. Theoret. Phys. (Kyoto) **11**, 309 (1954).
[19] T. K. McCubbin and W. M. Sinton, J. Opt. Soc. Am. **42**, 113 (1952).
[20] R. C. Ohlmann, P. L. Richards, and M. Tinkham, J. Opt. Soc. Am. **48**, 531 (1958).

large number of water vapor absorption lines, the monochromator case and the light pipes were evacuated.

Detector

The radiation was detected by a carbon resistance bolometer[21,22] operating at 1.3–1.5°K. This consisted of a $\frac{3}{16}\times\frac{1}{4}\times 0.015$ in. slab ground from a 56-ohm Girard-Hopkins resistor onto which indium contacts were evaporated. It was glued to the brass bottom of the light pipe with a 0.001-in. Mylar film interposed for electrical insulation. A light cone was used to condense the radiation from the 0.43-in. i.d. light pipe onto the bolometer. The bolometer, which operated in vacuum, typically has a resistance of 250 kohm when conducting 9 μa and with the helium bath at 1.4°K.

Temperature Measurement and Control

To observe the temperature dependence of the antiferromagnetic resonance, the FeF_2 sample was placed in the light pipe 12 in. above the bolometer. As the helium level dropped, the sample temperature rose at about 0.2°/min, which was slow enough so that the effect of the temperature change was negligible during a single sweep through the resonance line. This was checked by using the heater to hold the sample temperature constant during some runs. Sample temperatures of over 100°K could be obtained using the heater when the helium was at the bolometer level. The temperature was measured using a thermocouple made from a silver-gold alloy vs a gold-cobalt alloy.

Sample Preparation

A number of single-crystal samples were obtained[23] which were as large as several millimeters on their longest edge. Sample I, which was used for the majority of the experiments, was ground into a disk having the [001] direction, as determined by the usual Laue back-reflection technique, normal to its surface. This was done since the maximum resonance absorption of unpolarized light occurs when the direction of propagation is down the c axis, the easy axis of magnetization. Thicknesses of 2, 1, and 0.5 mm were used in successive groups of observations. It seemed impractical to grind this sample thinner than 0.5 mm since an excessive number of cracks and pinholes developed.

Sample II, which was 1 mm thick, was used primarily for the observations of the splitting of the resonance line using a magnetic field directed along the c axis. Since the nature of our apparatus required that the field be perpendicular to the direction of radiation propagation, the c axis had to lie in the plane of the sample disk. However, after the sample was mounted, the x-ray pattern disclosed that the c axis was 5° out of this plane. This error required a 0.4% correction to the effective magnetic field.

Preliminary results with a number of unoriented samples were also included in the resonance-frequency data. These were taken before improvements in the radiation purity were made, but were consistent with the later results.

IV. EXPERIMENTAL RESULTS

Field-Free Resonance

The antiferromagnetic resonance was observed at temperatures ranging from 1.5° to 66°K with no static magnetic field applied. Figure 4 shows the appearance of the data taken at the sample temperatures of 2°, 36°, and 50°K. The distribution of the background energy with wavelength is shown by the dashed lines in the figure. This is the energy which would have reached the detector in the absence of any antiferromagnetic resonance absorption. It was obtained with the sample heated to 100°K, well above the Néel temperature

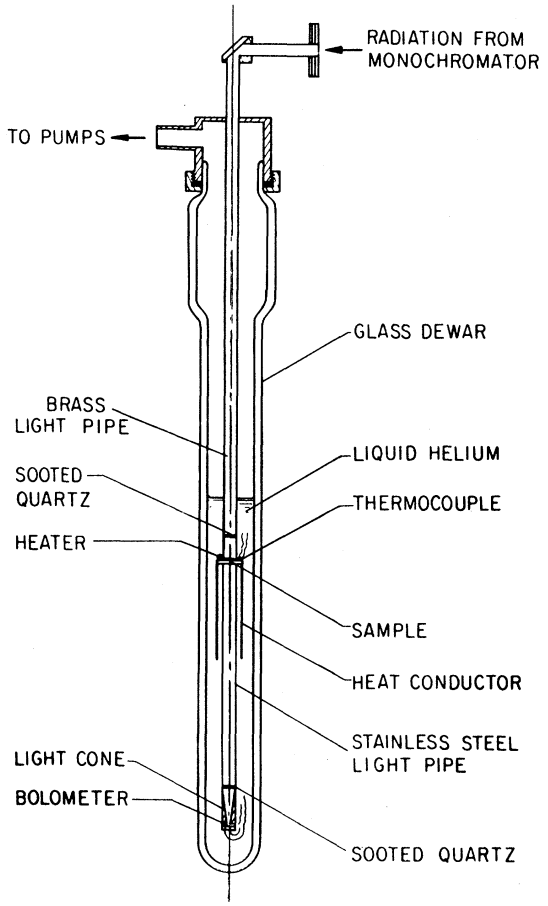

FIG. 3. The liquid-helium Dewar containing the FeF_2 sample and the bolometer detector. The surrounding Dewar filled with liquid nitrogen is not shown.

[21] W. S. Boyle and K. F. Rodgers, J. Opt. Soc. Am. **49**, 66 (1959).
[22] P. L. Richards and M. Tinkham, Phys. Rev. **119**, 575 (1960).
[23] We are indebted to Professor J. W. Stout for providing us with these samples.

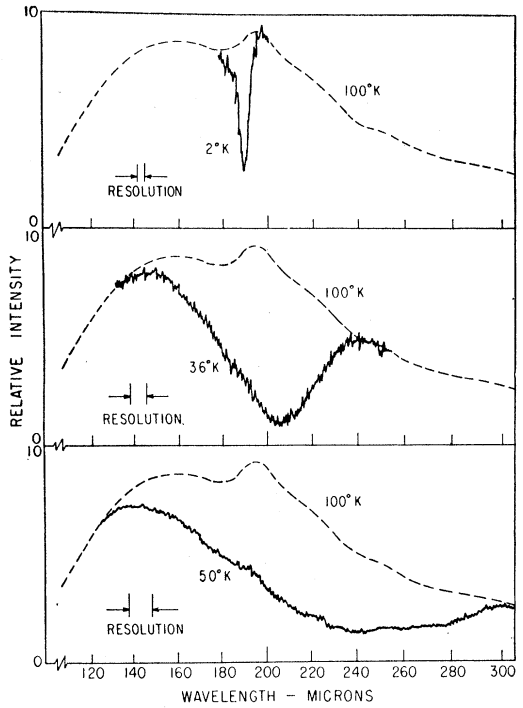

FIG. 4. Antiferromagnetic resonance lines. The original data has been replotted to have the three curves of equal scale, and the amplitude has been adjusted to have the absorption curves join smoothly on the background energy distribution shown by the dashed curve. These curves have been obtained using sample I, 0.5 mm thick, with the 260-μ grating in the spectrometer. Running conditions were: 2°K, 1.5-mm slit, 0.75 μ/min, 45-sec time constant; 36°K, 6 mm slit, 6 μ/min, 11-sec time constant; 50°K, 10 mm slit, 12 μ/min, 11-sec time constant.

(79°K). The shape of this distribution was the combined result of the source distribution, the grating efficiency, the filtering, including the filtering of the sample itself, and any false energy present. It was necessary to have the sample present in determining the background in order to separate the resonance absorption from the frequency-dependent lattice absorption. Evidence that the absorption line did not come from the excitation of a lattice vibrational mode is the splitting of the line produced by a magnetic field and also the temperature dependence of the resonance frequency. Large fluctuations on the background, due to interference phenomena from multiple internal reflections, were eliminated by nonparallel grinding of the two surfaces of each filter and of the sample. The slight irregularities remaining in the background distribution, which were also found with no sample present, were suspected to be due to stray reflections in the monochromator, but we were unable to eliminate them.

In normalizing these curves, the false energy simply was assumed to be a constant percentage of the background energy. This percentage was obtained from the fact that the attenuation at the line center was so high that, except for the widest lines observed, the true transmission at the center of the line was essentially zero. Thus the remaining signal (10–15% of the background energy) was false energy. This was confirmed by the observation that the resonance lines using sample I, between 15° and 45°K, which show at least a factor of 5 in their range of apparent linewidths, all had the same maximum absorption. Only the lack of instrumental resolution prevented the narrow lines observed below 15°K from showing the same maximum absorption.

After each curve was normalized, the resonance frequency was taken to be the frequency at which the relative transmissivity was a minimum. A plot of these frequencies vs temperature is shown in Fig. 5 along with the theoretical curve obtained below. The indicated uncertainties were estimated from the normalized transmission curves, and range from 10 to 30% of the linewidths. Since the observed lines were considerably asymmetric, the relationship between the frequency at the transmission minimum and the theoretical resonance frequency must be determined and this is done below in Sec. VI. However, for the very narrow lines, the difference is unobservable and the resonance frequency extrapolated to 0°K is

$$\tilde{\nu}_0(0)=52.7\pm0.2\ \text{cm}^{-1}. \quad (2)$$

Resonance Observations in a Magnetic Field

The observations in a magnetic field were necessarily made under a relatively narrow range of experimental conditions since only 19 000-oe fields were available compared to the effective internal field of 500 000 oe. At absolute zero, if the external field is along the preferred axis, the splitting of the resonance line[2,3] is twice the Larmor frequency $\omega_L=\gamma H_0$. This yields a splitting of about 4 cm^{-1} with the above field and with a spectroscopic splitting g factor equal to 2. Approximately, this splitting was observed at low temperatures where the linewidths were about one cm^{-1}. However, if the external field is perpendicular to the preferred axis, the splitting is a second-order effect equal to ω_L^2/ω_0. This would be

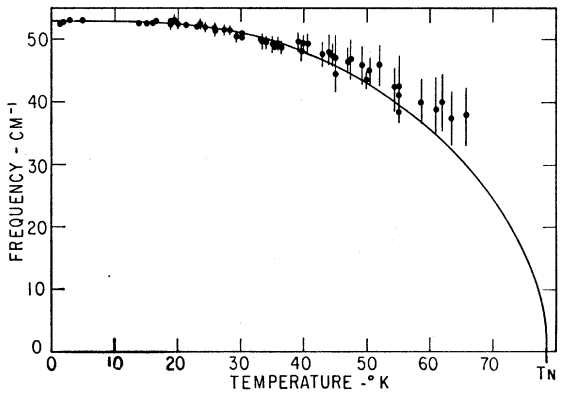

FIG. 5. Temperature dependence of the resonance frequency. The experimental points represent the frequencies at the transmission minima, and the curve is the result of the theory given in Sec. V.

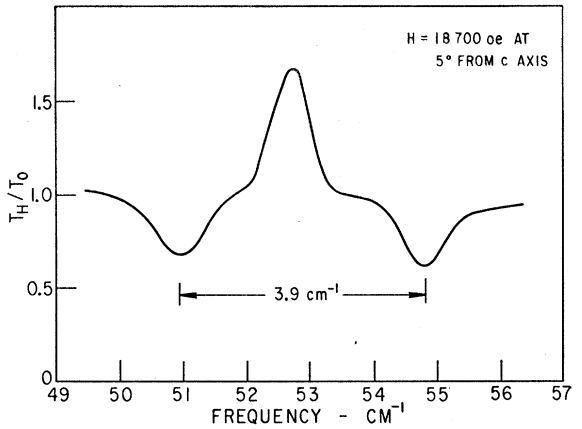

FIG. 6. Splitting of the line in a magnetic field. The ratio of the signal observed with the field on to that with the field off is plotted vs frequency. The central peak represents the inverse of the absorption observed in the absence of a field. The temperature was 1.5°K. The splitting is consistent with $g=2.25\pm0.05$.

only 0.08 cm^{-1} with the above fields and, therefore, it is unobservable.

The ratio of the signal from a typical run with an 18 700±400 oe field applied to that from a zero-field run is plotted in Fig. 6. Since all other conditions of the runs were identical, this ratio isolates the magnetic effects. The central peak represents the reciprocal of the zero-field absorption line, while the two dips on either side are the split lines which result from the field being present. The intensities of the lines are consistent with the assumption that, at the peak of each line, there was almost 100% absorption of the appropriate component of the radiation polarized perpendicular to the c axis, while the other component was not absorbed.

The result of these observations is that

$$g_{\parallel}=2.25\pm0.05. \quad (3)$$

This value agrees within experimental error with that obtained by Foner[17] from the susceptibility at high temperatures and with Tinkham's value from paramagnetic resonance observations on the dilute salt (Fe^{++} in ZnF_2).[24]

H_E, H_A, and K at $T=0$

As a preliminary to the discussion of the antiferromagnetic nature of ferrous fluoride, the values of some of the macroscopic parameters at absolute zero are calculated. The theory just discussed, including the appropriate modifications for the anisotropic g factor, is sufficient for this purpose. This means that Eq. (1b) should be written $\omega_0=\gamma_{\parallel}(2K/\chi_{\perp})^{\frac{1}{2}}(g_{\perp}/g_{\parallel})$, where $\gamma_{\parallel}=g_{\parallel}e/2mc$. We have used $g_{\perp}=2.05\pm0.05$, which was obtained from the high-temperature susceptibility data.[17] This value agrees with the value calculated from the susceptibility anisotropy,[16] $\chi_{\parallel}-\chi_{\perp}$, which also follows a Curie-Weiss law with a Curie constant proportional to $g_{\parallel}^2-g_{\perp}^2$.

[24] M. Tinkham, Proc. Roy. Soc. (London) **A236**, 535 (1956).

In the formalism of an isotropic g equal to $g_{\parallel}$, the effective field for resonance at $T=0$ is $\omega_0(0)/\gamma_{\parallel}=H_{\rm eff}(0)=500$ koe. By using $\chi_{\perp}(0)=0.0159M$ emu,[16] one obtains

$$K(0)=2.4\times10^9 \text{ ergs/mole}=1.1\times10^8 \text{ ergs/cm}^3. \quad (4)$$

Since only a small portion of the anisotropy arises from the interactions between the magnetic ions, while the major part is due to the interaction of each ion with its crystalline field, it is relevant to refer to the anisotropy energy per Fe^{2+} ion, $\kappa(0)$, which equals $K(0)/(N/2)$ or 40±2 cm^{-1}/ion. [We divide by $(N/2)$ rather than N because only one sublattice at a time enters in the consideration of anisotropy energy, i.e., $\frac{1}{2}K\cos^2\theta_1=(N/2)\frac{1}{2}\kappa\cos^2\theta_1$.]

The saturation magnetization of a sublattice is $M(0)=\frac{1}{2}Ng_{\parallel}\mu_B\langle S\rangle_0=560$ gauss (where we have taken $\langle S\rangle_0=0.98S$ to account for the zero-point motion). Thus one obtains $H_A(0)=K(0)/M(0)=200$ koe and $H_E(0)=540$ koe.

V. INTERPRETATION OF RESULTS

Origin of the Anisotropy

The principal source of magnetic anisotropy in FeF_2 is the effect of the asymmetry of the crystalline electric field upon the spins, the interaction occurring via the spin-orbit coupling. The other sources of anisotropy usually considered[14]—the dipolar interaction and the anisotropic exchange interaction—are probably an order-of-magnitude smaller. The dipolar anisotropy energy would be about the same as that found in MnF_2, which is magnetically and crystallographically similar to FeF_2 but whose anisotropy is almost entirely of dipolar origin. This energy (1.8 cm^{-1}/ion at 0°K[9,25–27]) is less than 5% of $K(0)$ found for FeF_2. The anisotropic exchange, resulting from the combined effect of spin-orbit coupling and the isotropic exchange, is more difficult to estimate. However, since it is a third-order perturbation, we might expect it to be small compared to the second-order crystalline field-spin-orbit-coupling interaction.

The free ion of Fe^{2+} has a $3d^6\ {}^5D$ ground state. The orthorhombic symmetry (D_{2h}) of the ligand field at the cation site in FeF_2 completely removes the fivefold orbital degeneracy of the D state. A quantitative calculation of the splitting is difficult[28–30] since it is sensitive to the polarizability of the fluorine ions and the degree of overlap of the d electrons onto the fluorine. However, the estimated separation of 1000 cm^{-1} between the ground state and the first excited orbital state is sufficiently greater than the free-ion spin-orbit-coupling constant,[31] $\lambda_0=-103$ cm^{-1}, that one may use a perturba-

[25] F. Keffer, Phys. Rev. **87**, 608 (1952).
[26] T. Oguchi, Phys. Rev. **111**, 1063 (1958).
[27] S. Foner, Phys. Rev. **107**, 683 (1957).
[28] K. Niira and T. Oguchi, Progr. Theoret. Phys. (Kyoto) **11**, 425 (1954).
[29] M. Tinkham, Proc. Roy. Soc. (London) **A236**, 549 (1956).
[30] T. Moriya, K. Motizuki, J. Kanamori, and T. Nagamiya, J. Phys. Soc. Japan **11**, 211 (1956).
[31] R. E. Trees, Phys. Rev. **82**, 683 (1951).

tion treatment on the ground state which leads to a spin Hamiltonian. For orthorhombic symmetry, the effect of an $\mathbf{L}\cdot\mathbf{S}$ perturbation may be represented in the spin Hamiltonian as

$$DS_z^2+E(S_x^2-S_y^2), \tag{5}$$

where only the lowest-order anisotropic terms are considered.

In the following analysis the molecular-field approximation is used to determine the relationships which exist between the parameters of the spin Hamiltonian and the macroscopic parameters entering into the antiferromagnetic resonance theory. The treatment has been simplified by neglecting the second term of Eq. (5), since Tinkham[24] has shown that $E\ll D$. Tinkham estimated that $D=-7.3\pm0.7$ cm^{-1} and $E=0.70\pm0.04$ cm^{-1} from his observation of paramagnetic resonance of Fe^{++} as a substitutional impurity in ZnF_2, combined with a measurement of the temperature-dependent anisotropic susceptibility of his dilute crystal.

The spin Hamiltonian for the whole crystal, involving the sum of the anisotropy contributions from each atom and the sum of all the exchange contributions, may be considerably simplified into a sum of the effective Hamiltonians of the individual ions by means of the molecular-field approximation. The exchange interaction is partitioned by replacing its effect on an individual ion by the interaction of the spin of that ion with the average spin on the rest of the lattice. The spin Hamiltonian may then be written, for an ion on site k of sublattice 1, as

$$\mathcal{H}_k=[2J_1z_1\langle\mathbf{S}_2\rangle+2(J_2z_2+J_3z_3)\langle\mathbf{S}_1\rangle]\cdot\mathbf{S}_k+DS_{kz}^2, \tag{6}$$

where $\langle\mathbf{S}_1\rangle$ and $\langle\mathbf{S}_2\rangle$ are the statistical averages of the spins of the individual ions on the two sublattices, and z_1, z_2, and z_3 are the coordination numbers of the various types of neighbors, namely 8, 2, and 4 in the FeF_2 lattice. In the absence of a magnetic field and below the transition temperature, we may let $\langle\mathbf{S}_2\rangle=-\langle\mathbf{S}_1\rangle$ as a sufficiently good approximation so that the above Hamiltonian may be written, dropping the k subscript, as

$$\mathcal{H}=-J\langle\mathbf{S}_1\rangle\cdot\mathbf{S}+DS_z^2, \tag{7}$$

where $J\equiv2J_1z_1-2J_2z_2-2J_3z_3>0$ and $D<0$.

Sublattice Magnetization

The sublattice magnetization[32] is found from the condition

$$\langle S_z\rangle=\mathrm{Tr}S_z\exp(-\mathcal{H}/kT)[\mathrm{Tr}\exp(-\mathcal{H}/kT)]^{-1}. \tag{8}$$

In the approximation used here, $\langle\mathbf{S}_1\rangle$ is directed in the positive z direction so that $\langle S_1\rangle=\langle S_z\rangle$. One obtains, using (7) and (8), the equation

$$\langle S_z\rangle=\sum m\exp(-E_m/kT)/\sum\exp(-E_m/kT), \tag{9}$$

where

$$E_m=-J\langle S_z\rangle m+Dm^2 \tag{10}$$

are the eigenvalues of the Hamiltonian and m covers the range of -2 to 2 for $S=2$. These equations determine $\langle S_z\rangle$ for a given J and D.

The transition temperature, T_N, is the highest temperature for which there is nonzero solution for $\langle S_z\rangle$. Setting the derivative with respect to $\langle S_z\rangle$ of each side of Eq. (9) equal at T_N, and letting $\langle S_z\rangle=0$, one obtains

$$kT_N/J=\sum m^2\exp(-Dm^2/kT_N)/\sum\exp(-Dm^2/kT_N) \tag{11}$$

$$\cong2+2.8(-D/kT_N)+0.6(-D/kT_N)^2+\cdots. \tag{12}$$

The effect of correlation, as calculated by Brown and Luttinger[33] and Smart[34] for $S=2$ and eight nearest neighbors, is to reduce the value of kT_N/J by about 15% and this correction has been included in the numerical determination of J.

Anisotropy Energy

The magnetic anisotropy energy is that part of the free energy which depends upon the direction which the sublattice magnetization, or $\langle\mathbf{S}\rangle$, makes with the crystal axes. Let $\langle\mathbf{S}\rangle$ be directed along an axis ζ, taken for convenience to lie in the xz plane and having direction cosines α, β, and γ with the x, y, and z axes. Then, for small values of α, the eigenvalues of the Hamiltonian (7) may be written

$$E_m=E_m^0+\tfrac{1}{2}E_m''\alpha^2. \tag{13}$$

Expanding the free energy per ion

$$f=-kT\ln[\sum\exp(-E_m/kT)]$$

in a Taylor's series in α, i.e., $f_0+\frac{1}{2}\kappa\alpha^2$, gives the anisotropy energy per ion κ as

$$\kappa\equiv K/(N/2)=\sum E_m''\exp(-E_m^0/kT)/\sum\exp(-E_m^0/kT). \tag{14}$$

The eigenvalues of the Hamiltonian are easily obtained by rotating to a new set of orthogonal axes ξ, η, and ζ and considering the term depending on angle as a perturbation. We obtain, including all terms to α^2,

$$E_m^0=-J\langle S_\zeta\rangle m+Dm^2, \tag{15}$$

$$E_m''=-D[3m^2-S(S+1)]+2D^2\left\{\frac{(m+\frac{1}{2})^2[S(S+1)-m(m+1)]}{J\langle S_\zeta\rangle-D(2m+1)}-\frac{(m-\frac{1}{2})^2[S(S+1)-m(m-1)]}{J\langle S_\zeta\rangle-D(2m-1)}\right\}. \tag{16}$$

[32] A similar calculation of the sublattice magnetization has been performed by A. Honma [J. Phys. Soc. Japan **15**, 456 (1960)].

[33] H. A. Brown and J. M. Luttinger, Phys. Rev. **100**, 685 (1955).

[34] J. S. Smart, J. Phys. Chem. Solids **11**, 97 (1959).

The anisotropy energy may be calculated as a function of temperature from Eqs. (14)–(16). We assume that $\langle S_\xi\rangle=\langle S_z\rangle$, which is calculated by Eqs. (9) and (10). At $T=0$, with $\langle S_\xi\rangle=S=2$, we have

$$\kappa_c(0)=E_m''|_{m=S}=-6D(1-\tfrac{3}{2}D/J)^{-1}, \qquad (17)$$

where the subscript on κ denotes that it is that part of the total anisotropy energy which is due to crystalline field-spin-orbit-coupling interaction. This method of obtaining the anisotropy energy is similar to that used by Yosida[4] for $|D|\ll J$, and has been treated for the case of large anisotropy and $S=1$ by Cooper.[35]

An estimate of D and J may be obtained from Eqs. (11) and (17), using $T_N=78.4°K$ and the value of $\kappa(0)=40.4\pm2$ cm^{-1} calculated using the antiferromagnetic resonance frequency. If we subtract 1.8 cm^{-1} of the anisotropy energy as being of dipolar origin, we obtain $\kappa_c(0)\approx38.6$ cm^{-1}. This gives $D=-10.5$ cm^{-1}, when J is increased by 15% to account for correlation. For comparison, Tinkham's value of $D=-7.3$ cm^{-1} would give $\kappa_c(0)=31.2$ cm^{-1}. This discrepancy suggests a larger anisotropy from other causes than was estimated. However, this low value of $\kappa_c(0)$ might also arise from the small difference in the lattice parameters of FeF_2 and ZnF_2 (the host lattice used by Tinkham), which affects both the crystal-field strength and the degree of overlap of the d electrons onto the fluorine ions. As a compromise, we have used $D=-9$ cm^{-1} in the calculation of the temperature dependence of the magnetization and anisotropy. For this value of D, we have $JS^2=101.2$ cm^{-1} and $\kappa_c(0)=35.4$ cm^{-1}. The exchange interaction between ions on different sublattices equals $2J_1z_1S^2=g\mu_BH_E(0)S=116.8$ cm^{-1}. Since $J\equiv2J_1z_1-2J_2z_2-2J_3z_3$, the exchange interaction with ions on the same sublattice is approximately 15.6 cm^{-1}.

The temperature dependence of the sublattice magnetization, $M(T)/M(0)=\frac{1}{2}\langle S_z\rangle$, was calculated from Eqs. (9) and (10) and is shown in Fig. 7. Cooper[35] points out that if correlation is included, the shift to the right from the Brillouin-function curve for $|D|\ll J$ is approximately twice as great as that shown in the figure, assuming his results for $S=1$ may be carried over to this case. The temperature dependence of the anisotropy energy was calculated using Eqs. (14)–(16) and is also shown in Fig. 7 both for $|D|\ll J$ and for $|D|/kT_N=0.165$, which should approximate the situation in FeF_2.

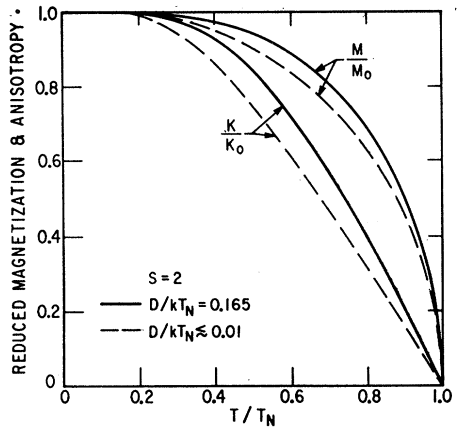

FIG. 7. Temperature dependences of the sublattice magnetization and the anisotropy energy constant. The curve for M/M_0 for small D is the usual modified Brillouin function for $S=2$.

The change of the antiferromagnetic resonance frequency with temperature has been determined using $K(T)$ and the experimental values of $\chi_\perp$ in Eq. (1b), and it is shown in Fig. 5. The experimentally observed resonance frequency decreases with temperature even more slowly than the molecular-field theory predicts, although the experimental uncertainty is considerable. The discrepancy may be qualitatively attributed to the neglect of correlation. In addition, there is also an effect due to the large linewidths observed at high temperatures. The theoretical calculation of the line shape, described in the following section, has shown us that, for the wide lines at $T>55°K$, the frequency at maximum absorption (plotted in Fig. 5) is up to several percent higher than that given by $\omega_0=\gamma(2H_EH_A+H_A^2)^{\frac{1}{2}}$. Unfortunately, the correction of the data for this effect could not be made reliably because of the limited accuracy of the linewidth data.

VI. LINEWIDTH AND SHAPE

The usual definition of the linewidth of a magnetic resonance line is the interval between the frequencies at which the absorption coefficient (or the imaginary part of the susceptibility) is half its maximum value. However, this quantity could not be directly obtained from the transmission measurements since the low transmission at the line center was not able to be measured accurately due to false energy and noise. In addition, in most cases the width of the line, as calculated in the following was less than the resolution limit of the spectrometer. Therefore, the observed transmission line shapes were fitted to theoretically calculated shapes, and the width of the theoretical line which best fit each observed line was considered to be its intrinsic linewidth.

As Dayhoff[36] has pointed out, regardless of the mechanism for the relaxation of the sublattice magnetizations, they must be expected to relax toward the instantaneous field acting upon them. Therefore, a damping term of the Landau-Lifshitz form was added to the equations of motion of $\mathbf{M}_1$ and $\mathbf{M}_2$, which then may be written, in the absence of a static magnetic field, as

$$\partial\mathbf{M}_{1,2}/\partial t=\gamma[\mathbf{M}_{1,2}\times\mathbf{H}_{1,2}-(C/M)\mathbf{M}_{1,2}\times(\mathbf{M}_{1,2}\times\mathbf{H}_{1,2})], \qquad (18)$$

where C is a dimensionless constant, and $M\equiv M_{1z}=-M_{2z}$. The components of the effective field acting

[35] B. R. Cooper, Phys. Rev. **120**, 1171 (1960).

[36] E. S. Dayhoff, J. Appl. Phys. **29**, 344 (1958).

on each sublattice are

$$\mathbf{H}_{1,2}=[-\lambda M_{x2,1}+H_x;\ -\lambda M_{y2,1}+H_y;\ \pm(H_E+H_A)], \quad (19)$$

where H_x and H_y are the components of the radiation field and $H_E=\lambda M$. Following the standard method,[8] the complex susceptibility was found. Since no static field has been included, the off-diagonal elements of the susceptibility tensor vanish. Letting $\chi_{xx}=\chi_{yy}\equiv\chi=\chi'-i\chi''$, we find that

$$\chi=\chi_\perp(\omega_0^2+iA\omega\delta)/(\omega_0^2-\omega^2+i\omega\delta), \quad (20)$$

where

$$\omega_0^2=\gamma^2(2H_EH_A+H_A^2)(1+C^2), \quad (21)$$

$$\chi_\perp=M/(H_E+\tfrac{1}{2}H_A), \quad (22)$$

$$\delta=2C\gamma(H_E+H_A), \quad (23)$$

$$A=(H_E+\tfrac{1}{2}H_A)/(H_E+H_A). \quad (24)$$

In the usual case $C\ll1$ so that ω_0 given by Eq. (21) is negligibly different from that given by Eq. (1). The dissipative component χ'' assumes a Lorentz form when $|\omega-\omega_0|\ll\omega_0$, namely,

$$\chi''\approx\chi_\perp(\omega_0/\delta)[1+(\omega-\omega_0)^2(2/\delta)^2]^{-1}, \quad (25)$$

having a full width at half-maximum equal to δ.

The transmission through the sample of thickness z, including reflection losses at each surface, is given by

$$T=\left[\frac{4n}{(n+1)^2+k^2}\right]^2\exp[-2(\omega/c)kz], \quad (26)$$

where

$$n-ik=[(1+4\pi\chi)\epsilon]^{\frac{1}{2}}, \quad (27)$$

and where ϵ is the complex dielectric constant. To isolate the magnetic effects, the relative transmissivity, T/T', where T' is the transmission when $\chi=0$, was calculated as a function of frequency using the constants appropriate to FeF_2, i.e., $4\pi\chi_\perp=0.009$/erg gauss^{-2} cm^{-3},

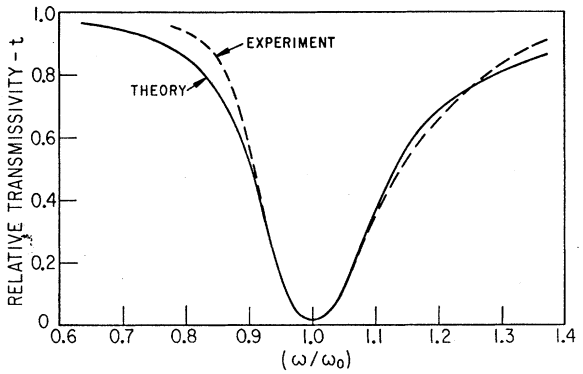

FIG. 8. A comparison of the experimental and theoretical line shapes. The experimental curve uses the normalized transmission from the 36°K run shown in Fig. 4, and the theoretical curve was calculated using $\delta/\omega_0=0.1$, where δ is the linewidth in angular frequency units. The agreement is within experimental error.

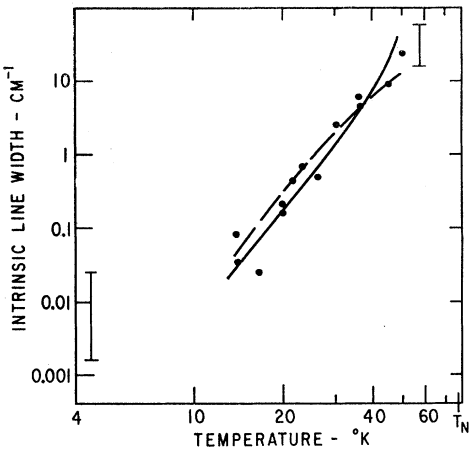

FIG. 9. The temperature dependence of the linewidth. The points are experimental. The solid curve was calculated from the theoretically obtained second moment assuming exchange narrowing. The dashed curve was calculated by relating the second and fourth moments to those of a cutoff Lorentz line shape.

$\epsilon=7-i0.05$, and $A=0.9$. The value of ϵ was estimated from the transmissivity found when the sample temperature was above the transition temperature. The calculated line shapes agree well with experiment for the observations above 25°K, as shown, for example, by Fig. 8. The lack of fit for the narrow lines at low temperatures is due to additional "spurious" absorption lines on the sides of the principal resonance.

The linewidths which were obtained by fitting the above theory to the observed transmission data, when plotted vs temperature as in Fig. 9, empirically were found to have a T^4 dependence. In the absence of a detailed theory of the relaxation at high temperatures, the linewidth was calculated by considering the fluctuations in the effective molecular fields, as suggested by Townes.[9] Since the resonant frequency ω_0 is proportional to $\kappa^{\frac{1}{2}}$, a statistically determined quantity, the moments of the line were obtained from the moments of κ. For example, the second moment of κ is

$$\langle(\Delta\kappa)^2\rangle_{\rm av}=\langle(E_m''-\kappa)^2\rangle_{\rm av}=(2\kappa/\omega)^2\langle(\Delta\omega)^2\rangle_{\rm av}. \quad (28)$$

Although, in principle, all the moments could be obtained and the line shape thus determined, two alternative approximate methods were used. One was to use only the second moment and assume the line was exchange narrowed. The linewidth δ is then given by

$$\delta=2\langle(\Delta\omega)^2\rangle_{\rm av}/\omega_{\rm ex}, \quad (29)$$

where the exchange frequency, $\omega_{\rm ex}$, is γH_E. The result of this calculation is shown by the solid curve in Fig. 9. In the other method of obtaining δ, the second and fourth moments of the line were calculated and equated to the second and fourth moments of a Lorentz line shape having an arbitrary cutoff. This gave the dashed curve in Fig. 9. The agreement of both methods with experiment is better than expected, considering the

fact that no adjustable parameters were used in either approach.

The weak satellite absorption lines on the side of the main resonance were barely observable with the resolution available. Therefore, a convolution of the transmission data was performed which effectively doubled the resolution. The instrumental resolution function was approximated by the energy distribution around the zero-order diffraction pattern. By successive approximations on a digital computer (IBM 650), the line shape was determined which, when convoluted with the resolution function, gave the observed line shape. To reduce the possibility that the satellite lines were due to "ghosts" in the background distribution, the line shape was normalized using a background distribution which also had been convoluted. The results of this computation are shown in Fig. 10. Although the integrated absorption of the strongest satellite was estimated as only 0.1–1.0% of the principal absorption, the sample was sufficiently thick to allow it to be seen.

VII. PARAMAGNETIC REGION

Above the transition temperature, the anisotropic terms in the spin Hamiltonian describe a number of low-lying energy states, between which magnetic-dipole transitions may occur with the absorption or emission of far-infrared radiation. The significance of the failure of our search for the absorption lines due to these transitions is discussed below.

If the exchange interaction in the paramagnetic region is neglected, a questionable assumption for FeF_2, the energy levels are given by the eigenvalues of the spin Hamiltonian, $DS_z^2+E(S_x^2-S_y^2)$, in an $S=2$ manifold. The result of this is a ground state doublet split by $-3E^2/D\approx 0.2$ cm^{-1}, and three higher states of energies approximately $-3(D+E)$, $-3(D-E)$, and $-4D$, respectively, above the ground state.[24] The transitions between the lowest two states and states 3 and 4 may be excited by x- or y-polarized radiation of frequencies 24.8 ± 6 and 29.4 ± 6 cm^{-1}, respectively, where we have set $D=-9\pm 2$ cm^{-1}.

A search for these lines, covering a frequency range of 13 to 70 cm^{-1}, both at 100° and 300°K, was conducted without success. We estimate that the lower limits on our ability to detect weak absorption lines was such that a relatively narrow line absorbing 15%, or a broad line absorbing 40%, would have been detected easily over the noise and background fluctuation. The absorption coefficient calculated from the transition probabilities of these transitions, assuming a Lorentz line shape, indicated that the lines would be unobservable if the relaxation time was less than 10^{-12} sec. This relaxation time is consistent with the observations of microwave Faraday rotation in FeF_2 by Teaney.[37] Such a rapid relaxation casts doubt on the simple paramagnetic theory. In FeF_2, the exchange energy is of the same order of magnitude as the energy level separations calculated above. Thus, rather than causing an exchange narrowing in the paramagnetic region, the exchange interaction may be expected to broaden the energy levels. If these broadened levels appreciably overlap, the eigenfunctions of the spin Hamiltonian neglecting exchange are poor approximations to the stationary states of the complete Hamiltonian.

[37] D. Teaney, thesis, University of California, Berkeley, California, 1960 (unpublished).

VIII. SUMMARY

Observations of antiferromagnetic resonance in FeF_2 have been made using far-infrared radiation at temperatures from 1.4° to 66°K ($\approx 0.8T_N$). The anisotropy and exchange energies have been calculated from the resonance frequencies and the static susceptibility, the anisotropy energy being an appreciable fraction of the exchange energy ($H_A/H_E=0.36$ at $T=0$). The large value of the anisotropy energy (1.1×10^8 ergs/cm^3 at $T=0$) is attributed primarily to the anisotropy of the crystalline electric field, which is coupled to the spin system via the spin-orbit interaction. The theoretical interpretation of the results was based on the molecular-field approximation, using an effective spin Hamiltonian which included the anisotropy. In this way, the macroscopic anisotropy energy was related to the anisotropy term in the Hamiltonian, DS_z^2, and we have estimated $D=-9\pm 2$ cm^{-1}.

The temperature dependences of the sublattice magnetization, the anisotropy energy, and the resonance frequency have been calculated and reasonably good agreement has been found with the experimental frequency vs temperature data. The line shapes were satisfactorily described by including a Landau-Lifshitz-type relaxation term in the resonance equations. Using this type of relaxation, we have calculated the intrinsic linewidths from the observed resonance linewidths. The observed T^4 dependence of these linewidths has been

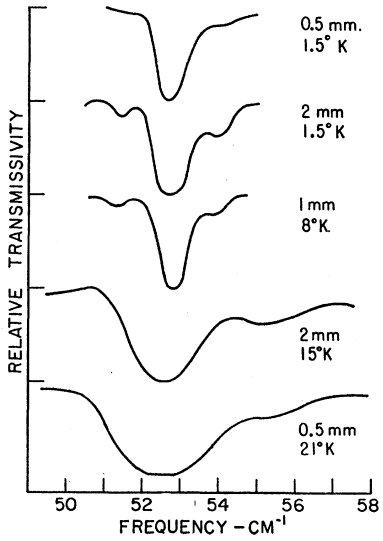

FIG. 10. Line structure at low temperature. The lines shown are the results after convoluting the resolution function from the original data which were taken using sample I.

fitted over a range of three decades by a theory based on the statistical fluctuations in the macroscopic anisotropy energy.

The success of the molecular-field approach in describing our results may be somewhat fortuitous. The separation of the complete Hamiltonian into relatively independent individual-ion Hamiltonians is a rough approximation, known to neglect the correlation of the spin directions of near ions. However, we have made full use of this approach in calculating the anisotropy, its temperature dependence, and the line widths. It is possible that the inclusion of the strong anisotropy, with its effect of aligning the spins along the preferred axis, partially compensates for the neglect of correlation.

ACKNOWLEDGMENTS

The authors wish to thank Professor F. Keffer, Dr. K. Yosida, Dr. R. Orbach, and Mr. B. R. Cooper, for many valuable discussions on the theoretical aspects of this paper. They wish to thank Professor J. W. Stout for providing the samples studied. Acknowledgment is also given to Mr. C. Grandt who aided in the mechanical design and construction of the far-infrared monochromator.

PHYSICAL REVIEW VOLUME 123, NUMBER 2 JULY 15, 1961

Gyromagnetic Ratio of Nickel Ferrite

G. G. Scott
Research Laboratories, General Motors Corporation, Warren, Michigan
(Received March 10, 1961)

The gyromagnetic ratio of the ferrite $NiOFe_2O_3$ was determined by measurements of the Einstein-de Haas effect. The g' value of 1.849 ± 0.002 indicates that the magnetization is largely due to the Ni^{++} ions as in the Néel model. Comparison with values of g determined by ferromagnetic resonance investigations furnishes evidence as to the validity of the Kittel-Van Vleck relation for ferrites.

INTRODUCTION

MAGNETOMECHANICAL determination of g factors for ferrites should furnish very direct evidence as to the source of the net magnetization in these materials. It was therefore thought that Einstein-de Haas experiments on a nickel ferrite would be of considerable interest.

The facility for making these measurements which has previously been reported[1] can be readily adapted for working with ferrites. In fact, for rods having length-to-diameter ratios of 15 to 1, many ferrites can be magnetized to the same order of intensity as the ferromagnetic metals with which we have previously been concerned. In addition, the high homogeneity which can be attained with ferrites reduces the random errors due to coupling with very small external fields.

The rod used in these experiments was made in the General Motors Research Laboratories. Considerable care was used to assure the stoichiometry of $NiOFe_2O_3$.

[1] G. G. Scott, Phys. Rev. **119**, 84 (1960).

RESULTS

These experiments on $NiOFe_2O_3$ were conducted on six different days. The values obtained on these days for g' were 1.849, 1.847, 1.845, 1.853, 1.850, and 1.848. Thus the magnetomechanical factor for this ferrite is 1.849 ± 0.002. The corresponding factors for Ni and Fe are 1.835 and 1.919, respectively. Hence it appears that the net magnetization in this material is largely due to the Ni^{++} ions as in the Néel model.

The g' value of 1.849 corresponds to a g value of 2.178. Resonance experiments by Yager, Galt, and Merritt[2] give a g value of 2.196 for $(NiO)_{0.95}(FeO)_{0.05}Fe_2O_3$. Also Yager *et al.*[3] obtain for $NiOFe_2O_3$ a g factor of 2.19. Hence these experiments also furnish evidence as to the validity of the Kittel-Van Vleck relation for ferrites.

The author wishes to thank the Charles F. Kettering Foundation for making available the specialized laboratory facilities required for conducting these experiments.

[2] W. A. Yager, J. K. Galt, and F. R. Merritt, Phys. Rev. **99**, 1203 (1955).
[3] W. A. Yager, J. K. Galt, R. F. Merritt, and E. A. Wood, Phys. Rev. **80**, 744 (1950).